NeuroImage 141 (2016) 416–430

Contents lists available at ScienceDirect

NeuroImage

journal homepage: www.elsevier.com/locate/ynimg

Tracking cognitive processing stages with MEG: A spatio-temporal model of associative recognition in the brain

Jelmer P. Borst [a,c,*], Avniel S. Ghuman [b], John R. Anderson [c]

[a] University of Groningen, Netherlands
[b] University of Pittsburgh, United States
[c] Carnegie Mellon University, United States

ARTICLE INFO

Article history:
Received 25 February 2016
Accepted 1 August 2016
Available online 4 August 2016

Keywords:
Associative recognition
Processing stages
Classification
ACT-R
MEG

ABSTRACT

In this study, we investigated the cognitive processing stages underlying associative recognition using MEG. Over the last four decades, a model of associative recognition has been developed in the ACT-R cognitive architecture. This model was first exclusively based on behavior, but was later evaluated and improved based on fMRI and EEG data. Unfortunately, the limited spatial resolution of EEG and the limited temporal resolution of fMRI have made it difficult to fully understand the spatiotemporal dynamics of associative recognition. We therefore conducted an associative recognition experiment with MEG, which combines excellent temporal resolution with reasonable spatial resolution. To analyze the data, we applied non-parametric cluster analyses and a multivariate classifier. This resulted in a detailed spatio-temporal model of associative recognition. After the visual encoding of the stimuli in occipital regions, three separable memory processes took place: a familiarity process (temporal cortex), a recollection process (temporal cortex and supramarginal gyrus), and a representational process (dorsolateral prefrontal cortex). A late decision process (superior parietal cortex) then acted upon the recollected information represented in the prefrontal cortex, culminating in a late response process (motor cortex). We conclude that existing theories of associative recognition, including the ACT-R model, should be adapted to include these processes.

Introduction

Associative recognition is the important ability to recognize that two events occurred at the same time, and might therefore be related. To investigate associative recognition memory, subjects are typically first asked to study pairs of words or other items, and later tested on whether two items were presented as a pair or not. Thus, associative recognition does not only involve judging whether an item was encountered before (recognition), but also whether it was encountered together with a specific other item (association).

Over the last four decades, an influential model of associative memory was developed, culminating in a computational simulation model in the cognitive architecture ACT-R (adaptive control of thought-rational; e.g., Anderson and Bower, 1973; Anderson, 1983; Anderson and Reder, 1999; Schneider and Anderson, 2012). This model was first based on behavioral data alone, but since 2003 it has also been evaluated and constrained by fMRI data (Danker et al., 2008; Sohn et al., 2005, 2003). The drawback of both behavior and fMRI is that they provide a single, aggregate measure of associative recognition (a single response or a single scan). This contrasts with the detailed ACT-R model that assumes cognitive steps in the order of 50 ms.

To improve our understanding of how associative recognition unfolds over time, we recently conducted an EEG experiment (Borst et al., 2013). The EEG data – with their high temporal resolution – suggested several changes to the model: whereas the original model assumed a single memory process and a brief decision stage, the EEG analyses provided evidence for two different memory processes and suggested a more complex decision process (Anderson et al., 2016; Borst and Anderson, 2015a). Unfortunately, the spatial resolution of the EEG setup was too coarse to localize cognitive processes in the brain.

In the current study we therefore conducted a MEG (magnetoencephalography) experiment of associative recognition. The combination of MEG's excellent temporal resolution (1 kHz) and reasonable spatial resolution (in the order of 1 cm; Hansen et al., 2010) should ground the model at a much finer scale in the brain, both temporally as well as spatially. We analyzed the MEG data with two complementary techniques: a traditional mass-univariate analysis, controlling for multiple comparisons by means of a non-parametric cluster analysis (Maris and Oostenveld, 2007), and a multivariate machine-learning classifier (e.g., Ghuman et al., 2014; Hirshorn et al., 2016; Pereira et al., 2009; Sudre et al., 2012).

* Corresponding author at: University of Groningen, Artificial Intelligence, Nijenborgh 9, 9747AG Groningen, Netherlands.
E-mail addresses: j.p.borst@rug.nl (J.P. Borst), ghumana@upmc.edu (A.S. Ghuman), ja+@cmu.edu (J.R. Anderson).

http://dx.doi.org/10.1016/j.neuroimage.2016.08.002
1053-8119/

In the remainder of this introduction, we will briefly discuss theories of associative recognition and the ACT-R model, followed by a description of the current study.

Theories on associative recognition

To account for *single-item* recognition memory, two classes of theories have been developed: single- and dual-process theories. Both classes have later been extended to explain associative memory (for reviews, see Diana et al., 2006; Malmberg, 2008; Wixted, 2007; Yonelinas, 2002). Single-process theories assume a single memory stage between perception and response, whereas dual-process theories assume two different memory stages.

Single-process theories are known as 'global matching' or 'signal detection' models (e.g., Gillund and Shiffrin, 1984; Hintzman, 1988; Malmberg, 2008; Murdock, 1993; Wixted, 2007; Wixted and Stretch, 2004). In these models, a 'compound cue' that contains both to-be-judged items is compared to all relevant traces in memory. If the combined similarity to all memory traces exceeds a certain criterion, it is assumed that the items were studied together. Thus, according to single-process theories there is only a single memory stage, and no information content is retrieved during this stage. Rather, a continuous index of the similarity to all memory traces is retrieved.

In contrast to single-process theories, dual-process theories describe associative recognition as a combination of two memory processes (e.g., Diana et al., 2006; Malmberg, 2008; Rugg and Curran, 2007; Yonelinas, 2002). An early, fast, and automatic familiarity process is similar to the matching process described above: it gives a continuous estimate of how familiar an item is. However, this information is typically assumed to be insufficient to judge associations. For this, a second process is required: recollection. This process is slower than the familiarity process and retrieves qualitative information from memory – including associative information. The familiarity and recollection processes have been related to different ERP components (e.g., Rugg and Curran, 2007). Familiarity is thought to elicit a negative response between 300 and 500 ms over mid-frontal electrodes, with new items being more negative than studied items (the FN400 or mid-frontal old/new effect). Recollection is characterized by a more positive signal for studied items than for new items between 500 and 800 ms over parietal electrodes (the parietal old/new effect).

ACT-R model

Unlike the theories described so far, the ACT-R model was directly developed to account for associative recognition. The model assumes four major sequential processing stages in associative recognition: perceptually encoding the items, retrieving a memory trace, making a decision based on the retrieved memory, and issuing a response (Fig. 1, top). Thus, like single-process theories it only assumes a single memory process. However, unlike single-process theories, this memory process retrieves qualitative information about the content of the memory, and is in that sense comparable to the recollection process of dual-process theories. The ACT-R model has been used successfully to explain latency, accuracy, and fMRI data of associative recognition tasks (e.g., Anderson and Reder, 1999; Danker et al., 2008; Schneider and Anderson, 2012; Sohn et al., 2005).

In the associative recognition experiment that we discuss below, participants were asked to study 32 word pairs in a training phase (e.g., "JELLY-MOTOR" or "COMFORT-MUSTARD"). In a subsequent test phase, they were again presented with word pairs, and had to judge whether they learned these pairs (targets; "JELLY-MOTOR") or whether the words were re-arranged (re-paired foils; "JELLY-MUSTARD"). Because foils were alternative pairings of the trained words, subjects needed to take the associative information of the words into account.

To perform this task, the ACT-R model starts by encoding the word pair from the screen. Next, it uses the encoded pair to retrieve the best matching word pair from memory (word pairs are stored as a single chunk of information in memory during the study phase; see Anderson and Reder, 1999, for details). In a short decision stage the model then compares the retrieved word pair to the pair on the screen. If the pairs match, the model decides that it learned the pair. If they do not match, the model decides it did not study the pair. Based on the decision, it issues the corresponding response in the final stage. Thus, also in the case of foils the model makes a retrieval based on the encoded words. Because the combination of encoded words does not exist in memory, a word pair containing only one of the words on the screen is retrieved instead. This pair is compared to the pair on the screen, which is different and consequently rejected as a target. This recall-to-reject process is consistent with a wide range of data on associative recognition (Anderson and Reder, 1999; Malmberg, 2008; Rotello and Heit, 2000; Rotello et al., 2000; Schneider and Anderson, 2012).

The model was implemented as a computational simulation in the cognitive architecture ACT-R (Anderson, 2007). It can be presented with the same information as human participants, and will yield reaction times, accuracy, and fMRI predictions that can be compared to human data (Borst and Anderson, 2015b; Borst et al., 2015). Two important effects in associative recognition data are the target-foil effect and the effect of associative fan. The target-foil effect refers to the observation that foil pairs are responded to slower than targets, if foils consist of the same *items* as targets, which is the case in the current experiment. Associative fan refers to the number of other items each word is associated to in memory, which, in the case of the experiment, is the number of pairs a word appears in. Pairs consisting of words with a higher associative fan are responded to slower than pairs with a lower fan status (for reviews, see Anderson, 2007; Anderson and Reder, 1999).

The ACT-R model accounts for both effects by means of a spreading activation mechanism. When issuing the memory retrieval in the associative retrieval stage, activation is spread from the encoded words to the word pairs in memory. In case of targets, both words of a pair in memory receive spreading activation. However, in the case of foils, only one of the words of a pair receives activation, because a pair containing both words does not exist in memory. As a result, foil pairs receive less activation and are retrieved slower than target pairs. The fan effect is explained in a similar manner: It is assumed that the spreading activation from the encoded words is a fixed amount, but in case of higher fan words has to be divided over multiple word pairs. That is, if

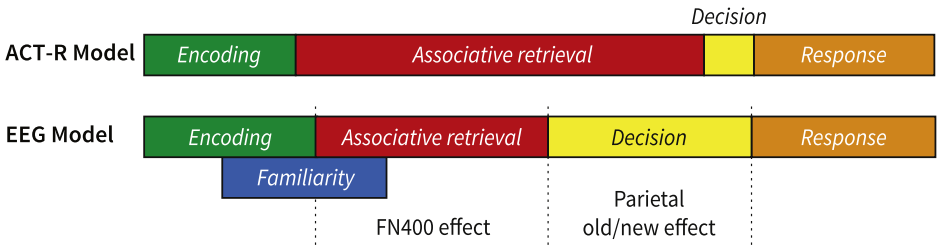

Fig. 1. Processing stages in the ACT-R model (top) and in the adapted model of Borst & Anderson (2015a). Adapted with permission from Borst & Anderson (2015a).

an encoded word occurs in multiple pairs in memory (higher associative fan), the spreading activation is divided over these pairs. As a result, pairs with higher-fan words receive less spreading activation, and are therefore harder to retrieve. For a detailed treatment, including the underlying equations and quantitative predictions, see Anderson and Reder (1999) or Schneider and Anderson (2012).

The ACT-R model does not only account for response times and error rates, but is also able to quantitatively account for fMRI data in several brain regions (Danker et al., 2008; Sohn et al., 2003, 2005). Most importantly, a region in the left prefrontal cortex is sensitive to the fan-status of associative recognition items, with higher-fan items resulting in greater BOLD activation. In addition, the same region was found to be more active in response to foils than to targets (Lepage et al., 2003). This region is thought to reflect retrieval of the word pairs from memory (Anderson, 2007; Borst and Anderson, 2015b), as the activity patterns match the slower retrievals of higher-fan items and foils in the model.

EEG findings

The ACT-R model has been very successful in explaining behavior and fMRI data (e.g., Anderson and Reder, 1999; Schneider and Anderson, 2012; Sohn et al., 2005). However, both behavior and fMRI provide an aggregate measure of the complete associative recognition process. Recently, we therefore conducted an associative recognition study with EEG, which can measure the neural processes at a millisecond resolution throughout the recognition process (Borst et al., 2013). We analyzed the data with traditional methods and with two different classification approaches (Anderson et al., 2016; Borst and Anderson, 2015b), which resulted in the 'EEG model' in Fig. 1 (bottom). In this model, a familiarity stage begins after some encoding has occurred, and extends partly into an associative recollection process. The recalled evidence is maintained for the decision process, and results in a sustained response whose amplitude is related to the activation of the memories (Anderson et al., 2016). In addition, the duration of the decision process depends on the recalled evidence (Borst and Anderson, 2015a).

Thus, in contrast to the original ACT-R model, the EEG analyses indicated the existence of two memory stages: a familiarity stage and a recollection stage. In addition, the analyses suggested a complex decision stage that processed the input from the recollection process to make a decision, and that is sensitive in duration both to target/foil status as well as to associative fan.

Current study

With the current study we want to shed more light on the neurodynamic processing stages of associative recognition and thereby further evaluate the ACT-R model and single- and dual-process theories. We aim to answer two questions: 1) are there one (ACT-R, single-process theories), two (EEG model, dual-process theories), or more memory processes involved in associative recognition, and 2) what is the nature, timing, and location of these processes?

To answer these questions, we conducted a MEG experiment consisting of two phases on consecutive days. In the training phase on day 1, participants were asked to study 32 word pairs. In the test phase on day 2, participants were again presented with word pairs, and had to judge whether they learned these pairs in the training phase or not. To aid the identification of processes involved in associative recognition, we manipulated four factors in the experiment: word length, associative fan, probe type, and response hand. Word length was expected to affect the encoding stage. Although it only has a negligible effect on reading speed (Juhasz and Rayner, 2003; Spinelli et al., 2005), it is reflected in early occipital signals (85 ms after stimulus onset) and later prefrontal signals (from 300 ms onwards; Borst et al., 2013; Hauk and Pulvermüller, 2004; Sudre et al., 2012; Van Petten and Kutas, 1990). Associative fan was expected to affect the duration of a retrieval stage, as discussed above. It is known to have a strong effect on the EEG signal both over prefrontal and parietal cortex (Borst et al., 2013; Heil et al., 1997; Khader et al., 2007; Nyhus and Curran, 2009). Probe type (targets and re-paired foils) should influence the decision process. Finally, response hand was varied between blocks (not between targets and foils), and should therefore be reflected exclusively in a response process (not in the decision process).

In addition to a univariate analysis, we used a multi-variate machine-learning classifier to analyze the MEG data and identify processing stages (e.g., Chan et al., 2011; Das et al., 2010; Pereira et al., 2009). Traditional univariate analysis methods are based on the assumption that the relevant information is coded in a single sensor, source (M/EEG), or voxel (fMRI) or in the average signal of a region, while it might as well be represented in the activity pattern across multiple sensors, sources, or voxels (Haynes and Rees, 2006; Norman et al., 2006). The current analysis was inspired by the work of Sudre and colleagues, who investigated where and when certain semantic categories are represented in the brain (Sudre et al., 2012). For the current study, we trained a classifier to identify the experimental conditions in 50-ms windows between stimulus and response. The idea is that if the classifier can distinguish between two conditions in a certain time period (e.g., left and right hand 100–150 ms before the response), one can conclude that information regarding response hand is present in the MEG signal, and consequently that a response process is underway. In addition, after projecting the MEG signal on the cortical surface (Gramfort et al., 2014; Hansen et al., 2010), we divided the surface in 68 regions-of-interest (ROIs) and trained the classifier on each region and each 50-ms time window separately. This results in even more fine-grained information, where the combination of condition, brain region, and time window can be used to infer the underlying process.

Method

The experiment consisted of two phases: a training phase in which subjects learned word pairs and a test phase in which subjects completed an associative recognition task. The test phase was scheduled the day after the training phase and took place in the MEG scanner. During the test phase subjects had to distinguish between targets and re-paired foils. Because foils were alternative pairings of the trained words, subjects needed to take the associative information of the words into account. Note that words always appeared in the same position of a pair, irrespective of target or foil status. In addition to probe type (target or re-paired foil), we manipulated word length (short or long), associative fan (words had either 1 or 2 associates), and response hand, resulting in 16 unique conditions. We used structural MRI images to estimate cortically-constrained minimum norm estimates (MNE; Gramfort et al., 2014) of the cortical currents underlying the measured MEG signal.

Subjects

Twenty individuals from the Carnegie Mellon University community completed the experiment. These subjects had performed an fMRI experiment in our lab previously, and gave permission to use their structural MRIs from the previous study to aid the MEG analysis. One subject fell asleep in the MEG scanner, and one performed more than two standard deviations below the mean performance rate (15% errors, where the other subjects scored on average 6% errors). This left 18 subjects for analysis (6 males and 12 females, ages ranging from 18 to 35 years with a mean age of 23.6 years). All were right-handed and none reported a history of neurological impairment. Written informed consent as approved by the Institutional Review Boards at Carnegie Mellon University and the University of Pittsburgh was obtained before the experiment. Participants received $65 compensation.

Materials

Word pairs were taken from Borst et al. (2013). For that study, word pairs were constructed from a pool of 464 words selected from the MRC Psycholinguistic Database (Coltheart, 1981). The words were nouns with word frequency between 2 and 100 occurrences per million and a minimum imageability rating of 300. Half of the words were 4 or 5 letters and composed the short word list, which had a mean word frequency of 24.3 occurrences per million ($SD = 22.1$), mean imageability rating of 539.3 ($SD = 55.3$), and mean word length of 4.5 letters ($SD = 0.5$). The other half of the words were 7 or 8 letters and composed the long word list, which had a mean word frequency of 24.4 occurrences per million ($SD = 23.4$), mean imageability rating of 505.6 ($SD = 81.6$), and mean word length of 7.2 letters ($SD = 0.4$). The 232 words of each length were divided randomly into two lists – a 24-word study list (which was re-used in the current study) and a 208-word new foil list (which was not used for the current study) – such that the lists were matched on word frequency, imageability, and word length according to t-tests (all $ps > 0.1$). Word frequency was also matched across the corresponding lists of each length, thereby avoiding the natural confound between word frequency and length. Study lists were also constrained such that each word started with a unique three-letter sequence.

The study lists were used to create two sets of probes: targets and re-paired foils. A set of 32 target word pairs was constructed from the study lists such that there were eight word pairs for each combination of length (short or long) and fan (1 or 2). Both words in short pairs were 4 or 5 letters and both words in long pairs were 7 or 8 letters. Each word in a fan-1 pair appeared only in that pair, whereas each word in a fan-2 pair appeared in two pairs. A corresponding set of 32 foil word pairs was constructed in a similar manner by recombining words from different target pairs of the appropriate length and fan. Thus, there were 8 conditions defined by the probes: probe type (target or re-paired foil), word length (short or long) and associative fan (1 or 2). These were combined with response hand to create 16 unique conditions. The randomization of words and their assignment to conditions were unique for each subject.

MEG recording

MEG data were recorded with a 306-channel Elekta Neuromag (Elekta Oy) whole-head scanner. The 306 channels are distributed into 102 sensor triplets, each containing one magnetometer and two orthogonal planar gradiometers. Data were digitized at 1 kHz. As part of standard MEG testing, four head position indicator (HPI) coils were attached to the subject's scalp to track the position of the head in the MEG helmet. The position of the HPI coils, three fiducial points (nasion, left and right pre-auricular), and an additional 30 to 60 scalp surface points were digitized to aid co-registration of the anatomical MRI and MEG sensors. In addition, we placed electrodes above, below, and next to the eyes to measure eye movements and eye blinks (EOG). After preparation, subjects were seated in a three-layer magnetically-shielded scanner room. Two response gloves (left and right) were placed on the table in front of the subjects, and attached to their wrists with velcro. The stimuli were projected onto a screen about 1 m in front of the subject. Timing accuracy was ensured by measuring stimulus onset with a photodiode that was directly connected to the MEG recording system.

Structural MRI

Structural MRIs were obtained during previous experiments in our lab. The images were acquired on a 3T Verio Scanner using a 32-channel RF head coil and an MPRAGE sequence (TR = 1700 ms, TE = 2.48 ms, flipangle = 9°, 256 × 256 matrix, FOV = 256 mm × 256 mm, 176 1 mm thick sagittal images).

Procedure

The training and test phase of the experiment were conducted on consecutive days. In the training phase subjects learned the target word pairs. The training phase started with each target word pair presented onscreen (one word above the other) for 5000 ms followed by a 500-ms blank screen. Subjects were instructed to read each pair and make an initial effort to memorize it. Following target presentation, subjects completed a cued recall task designed to help them learn the target word pairs. On each trial they were presented with a randomly selected target word and had to recall the word(s) paired with it (two-word responses were required for fan 2 words). The self-paced responses were typed and feedback in the form of the correct response was provided for 2500 ms following errors. If a target word elicited an error, it was presented again after all other target words had been presented. A block of trials concluded when all 48 target words had elicited correct responses. Subjects completed a total of three blocks of cued recall, and thus responded correctly three times to each word.

On the second day, subjects started with one additional block of cued recall to refresh their memories. Afterwards they were prepared for the scanner and completed the test phase in the scanner (Fig. 2). Each trial began with a centrally presented fixation cross for a variable duration sampled from a uniform distribution from 400 to 600 ms. Following fixation, a probe word pair appeared onscreen (one word above the other) until the subject responded with a keypress to indicate whether the probe had been studied during the training phase. In half the blocks subjects responded with their right hands, in the other half with their left hands. Left- and right-handed blocks were alternated; half of the subjects started with a right-handed block, the other half with a left-handed block. Targets required "yes" responses (left or right index finger) and foils required "no" responses (left or right middle finger). Response instructions (including hand) were repeated before each block. Subjects were instructed to respond quickly and accurately. Following the response, accuracy feedback was displayed for 1000 ms, after which a blank screen appeared for 500 ms before the next trial began.

Subjects completed a total of 14 blocks (7 left-handed, 7 right-handed) with 64 trials per block; each block contained all target and foil word pairs in random order. All 16 conditions thus occurred equally often, which resulted in 56 trials per condition during the test phase.

General analysis

For all analyses, except error rate, incorrect trials and trials with response times (RTs) longer than 10,000 ms were excluded. In addition, trials with RTs exceeding 3 *SD*s from the mean per condition and subject were excluded. In total, 2.3% of correct trials were removed, leaving on average 51.7 observations per condition per subject. To investigate behavioral data we used repeated-measure ANOVAs.

MEG analysis and cortical current estimation

MEG data were visually inspected to reject flat or noisy channels. Next, the FieldTrip toolbox (Oostenveld et al., 2011) for MATLAB was used to apply a band-pass filter (0.5–50 Hz) and subsequently down-

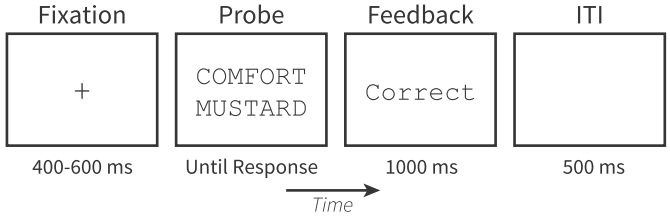

Fig. 2. Trial structure. ITI = inter-trial interval.

sample the data to 250 Hz. Eye blinks and saccades were removed by decomposing the MEG data into independent components with EEGLAB's (Delorme and Makeig, 2004) independent component analysis (ICA) algorithms as implemented in FieldTrip. Components were automatically marked for rejection if their correlation with either the horizontal or vertical EOG recordings was higher than 0.5 and these marked components were also manually inspected before rejection. The remaining components were projected back to sensor space. Finally, sensor data were realigned to the average head position of all subjects.

Stimulus-locked epochs of 1000 ms (including a 200-ms pre-stimulus baseline) were extracted from the continuous recording and baseline-corrected using the pre-stimulus interval. Response-locked epochs of 1000 ms (800 ms pre-response and 200 ms post-response) were also extracted from the continuous recording to examine late-occurring effects while controlling for variability in RTs. Response-locked epochs were baseline-corrected using the 200-ms pre-*stimulus* baseline. We excluded incorrect trials and trials with outliers in RTs as described above. In addition, stimulus- and response-locked epochs containing sensor-values exceeding 7.5 *SD*s from the mean per sensor and subject over all epochs were excluded from further analysis.

Because the measured magnetic signal does not directly indicate the location and magnitude of cortical currents, we projected the sensor data onto the cortical surface using cortically constrained minimum norm estimates (MNE; Gramfort et al., 2014). The MNE method attempts to find the distribution of currents on the cortical surface with the minimum overall power that can explain the MEG sensor data. To this end we first constructed 3D cortical surface models from the subjects' structural MRIs using FreeSurfer (Dale et al., 1999; Fischl, 2012). These cortical surface models were manually co-registered with the MEG data on the basis of the recorded fiducials and scalp surface points. Then, 2562 source dipoles were placed on the gray-white matter boundary of each hemisphere, approximately 6 mm apart, and a forward operator from these sources was calculated using a single compartment boundary-element model. A noise-covariance matrix was computed for each subject from 400 ms to 50 ms before stimulus presentation on each trial. The noise-covariance matrix and the forward operator were combined into a linear inverse operator (loose orientation constraint of 0.1, no depth weighting), which can be used to project sensor data onto the source dipoles on the cortical surface. The resulting three components (x, y, z) of each dipole were combined by taking the square root of the sum of squares, as is common practice in the MNE analysis method. The inverse operator was used to project the average stimulus- and response-locked epochs per subject and condition to the source space. These source estimates were then morphed onto the standard MNI brain using MNE's surface-based normalization procedure (Gramfort et al., 2014).

To compare conditions and identify time periods and source locations of interest while controlling for multiple comparisons, we applied nonparametric cluster-based permutation tests (Maris and Oostenveld, 2007). First, we contrasted the two levels of each condition and determined sources with $p < 0.01$. These sources were clustered based on time (adjacent time points) and space (Euclidian distance < 7 mm) over the whole brain and the entire 1300 ms interval. Next, t-values in each cluster were summed to create cluster-level statistics. To derive the empirical null distribution of the cluster-level statistic, we applied this procedure to 10,000 random permutations of the data for each condition, in which each condition level was labeled randomly for each subject (e.g., we calculated averages for long and short words for each subject, then randomly re-labeled these averages). The proportion of these permutations with a greater maximum cluster-level statistic than the cluster-level statistic of the original, non-permuted data was taken as the p-value for the original clusters. Clusters with a permutation p-value < 0.05 were considered significant.

Multivariate classifier

To track processing stages we applied a machine-learning classifier to the data,[1] following the methodology outlined by Sudre et al. (2012; see also Borst et al., 2013). To determine *when* certain information was present in the MEG signal we divided the sensor data into 50-ms intervals and performed binary classification for each experimental factor (e.g., long and short words) in these intervals. To also determine *where* the information was processed, we divided the source estimates into 68 regions-of-interest (ROIs) following the Desikan-Killiany atlas (Desikan et al., 2006; Freesurfer "aparc" annotation) and into 50-ms intervals. Again, we performed binary classifications for each factor in each interval and ROI.

Preparation

The classifier algorithm requires that trials be the same length. The data were therefore simultaneously stimulus- and response-locked, to capture effects occurring at both the start and the end of the trials in a single analysis. To this end, all trials were warped to a length of 1500 ms, composed of three parts: a 200-ms pre-stimulus baseline, the first 500 ms after stimulus onset, and a warped 800 ms. That is, we kept the first 500 ms of each trial intact and resampled the remaining data of each trial: the portion of each trial occurring after 500 ms was "shrunk" or "stretched" to a duration of 800 ms.[2] This approach preserved peaks in the MEG waveforms throughout the trial. This type of event-locking procedure has also been used to align individual trials of varying durations in fMRI experiments (Anderson et al., 2008), and was previously applied to our EEG dataset (Borst et al., 2013). To ensure that we did not introduce artifacts with this procedure, we additionally classified separately stimulus-locked and response-locked data. To this end, we excluded trials shorter than 700 ms, and extracted 900-ms epochs from the continuous recording (including a 200 ms pre-stimulus or post-response interval). All data were baseline-corrected using the 200 ms pre-stimulus intervals.

After stimulus- and response-locking the data, we created classifier examples by averaging over the 7 presentations of each unique word pair for left- and right-handed responses for each subject (we averaged over the presentations to decrease noise; cf. Borst et al., 2013; Sudre et al., 2012). This resulted in 8 examples for each of the 16 conditions formed by the factorial combination of fan, word length, probe type, and response hand, yielding 128 examples in total for each subject. Given that we used 1500-ms epochs,[3] the data were down-sampled to 250 Hz, and data were recorded at 306 sensors, this yielded $376 \times 306 = 115{,}056$ features per example, where each feature is a time point of a sensor. From the examples and features, we created a $128 \times 115{,}056$ matrix $\mathbf{X}$ for each subject. The final step in preprocessing the data was normalizing each sensor (over the different examples) in $\mathbf{X}$ to a standard deviation of 1. Each sensor was normalized separately to prevent channels with higher amplitudes from disproportionately influencing the classifier results. In addition to matrix $\mathbf{X}$, we also created a 128×4 matrix $\mathbf{Y}$ that contained the labels for the examples. The columns in $\mathbf{Y}$ coded fan (fan $1 = -1$ and fan $2 = 1$), word length (short $= -1$ and long $= 1$), probe (foil $= -1$ and target $= 1$), and response hand (right $= -1$, left $= 1$).

For the source space classification in the ROIs, we projected the 8 examples (averages of 7 presentations) of each condition onto the cortical surface as described above. Instead of 306 sensors, this yielded 5124 source estimates per time point, and therefore $376 \times 5124 = 1{,}926{,}624$ features per example. The matrix $\mathbf{X}$ measured therefore

[1] Matlab code to perform the sensor-based classification can be found on http://www.jelmerborst.nl/models.

[2] We resampled the remaining part of each trial using Matlab's *resample* function to a length of 800 ms. To minimize edge effects, we padded the start and end of each interval before resampling.

[3] The procedure is described for the stimulus-and-response-locked data; it was identical for the separate stimulus-locked and response-locked classifier analyses.

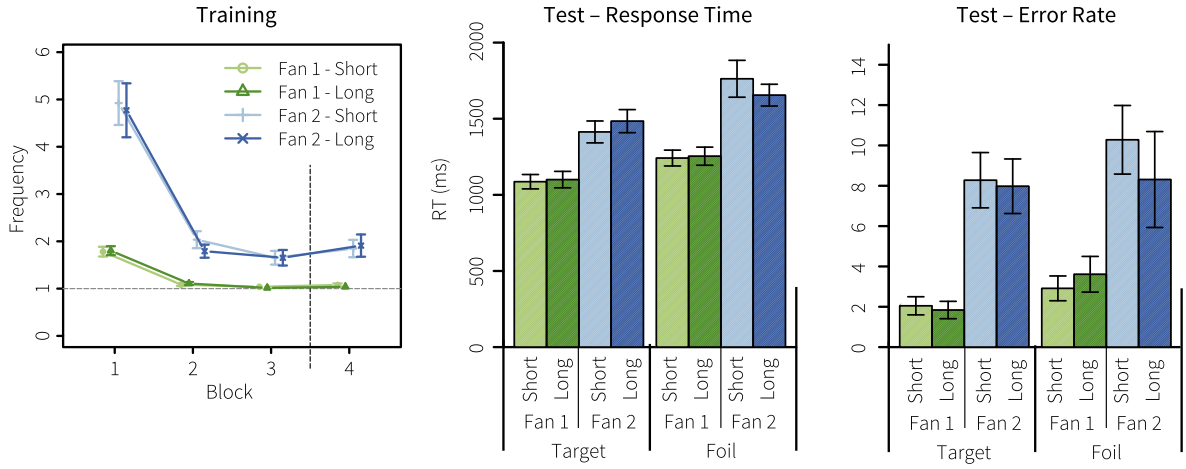

Fig. 3. Behavioral results of the training (left), test RT (mid), and test error rate (right). Error bars indicate standard errors. Data were not split out for right and left-handed responses, as there were no significant differences between response hands in behavior.

128 × 1,926,624 for each subject. Each source was then normalized analogously to the sensors before. Note that we performed the classification only on subsets of these 1,926,624 features as defined by the ROIs: the mean size of the ROIs was 67 sources, with 189 sources being the maximum. Thus, ROI classification was done on a maximum of 189 × 376 = 71,064 features per example.

Algorithm

To classify the data we used the machine-learning technique ridge regression (e.g., Hastie et al., 2001). In essence, ridge regression is a linear regression method that can handle situations with many correlated predictors, as is the case here. Ridge regression learns a mapping $\hat{\mathbf{W}}$ between the $n \times p$ example matrix $\mathbf{X}$ and the labels $\mathbf{Y}$:

$$\hat{\mathbf{W}} = \left(\mathbf{X}^T\mathbf{X} + \lambda \mathbf{I}_p\right)^{-1}\mathbf{X}^T\mathbf{Y} \quad (1)$$

$\mathbf{I}_p$ is the $p \times p$ identity matrix and λ is a complexity parameter that penalizes large coefficients $\hat{\mathbf{W}}$. Eq. (1) requires the inversion of a $p \times p$ matrix. Eq. (1) can be rewritten in its dual form:

$$\hat{\mathbf{W}} = \mathbf{X}^T\left(\mathbf{X}\mathbf{X}^T + \lambda \mathbf{I}_n\right)^{-1}\mathbf{Y} \quad (2)$$

in which $\mathbf{I}_n$ is the $n \times n$ identity matrix. The dual form requires the inversion of an $n \times n$ matrix rather than a $p \times p$ matrix. Given that $n = 128$ examples and $p = 115{,}056$ features per example (maximum) in our case, the dual form enables the algorithm to run considerably faster.

$\hat{\mathbf{W}}$ is a $p \times 4$ matrix where each column contains the weights for one of the four labels. These weights can be used to predict classes (e.g., fan 1 or 2) to which new examples belong by multiplying new examples $\mathbf{T}$ by $\hat{\mathbf{W}}$:

$$\hat{\mathbf{Y}} = \mathbf{T} \cdot \hat{\mathbf{W}} \quad (3)$$

$\hat{\mathbf{Y}}$ denotes the classification. In our case, the labels $\mathbf{Y}$ were either 1 or −1. Positive $\hat{\mathbf{Y}}$ were interpreted as a 1 classification (fan 2, long, target, left hand), and negative $\hat{\mathbf{Y}}$ as a −1 classification (fan 1, short, foil, right hand).

Training and testing the classifier

We trained and tested the classifier separately for each subject. This involved two steps. First, the best λ (the complexity parameter) was determined separately for each condition (thus, we used a different λ for each condition). Second, the classifier was evaluated. For both steps we used leave-one-out cross-validation (LOOCV). That is, we trained the classifier on 127 examples and used the resulting $\hat{\mathbf{W}}$ to classify the 128th example. We repeated this procedure for all examples, yielding 128 scores.

To determine the optimal value for λ, we used LOOCV to minimize the mean squared prediction error (MSE) separately for each label (fan, word length, probe type, hand):

$$MSE = \frac{1}{n}\sum_{i=1}^{128}(y_i - \hat{y}_i)^2 \quad (4)$$

where y_i is the label for example i and $\hat{y}_i$ is the raw classification value for that example. We searched for a value of λ between 0 and 1,000,000 in the following manner. First, MSEs were calculated for 11 linearly spaced values of λ between 0 and 1,000,000. Next, we calculated MSEs for 11 linearly spaced points spanning the interval that contained the value of λ that previously minimized MSE. We repeated this procedure until the improvement in MSE was smaller than 0.01. Once the optimal value of λ was determined, we ran the classifier once more using LOOCV to calculate final prediction accuracy (percentage of correct classifications), which is reported in the Results section.[4]

The sensor-based classifier was first trained on all data between −200 and 1300 ms to assess how well it could perform given all data. To determine when the different types of information were processed in the brain, we subsequently trained and tested the classifier using 50-ms windows. In the case of the source-based ROI classifier, we first trained on all data (all intervals) in an ROI to determine the neural correlates of the processes of interest. Next, we divided the data in an ROI into 50-ms intervals to investigate time and location simultaneously.

Results

Behavior

Training phase

Fig. 3, left panel, shows the frequency with which target words were presented during each block of the cued recall task. The minimum

[4] Note that this approach is sub-optimal, because the value of λ is determined on the same data as the predictions are made, albeit in separate LOOCV-iterations. Thus, the final test-set is not fully independent of the training set, possibly resulting in over-fitting of the data. As a solution, one can recompute λ on each iteration of the prediction-LOOCV. We applied this alternative approach to the MEG sensor data, and showed that the results are virtually identical (Supplementary Fig. S1). However, as this approach was computationally infeasible for the MEG source data and the results remained unchanged, we decided to use the procedure described in the main text.

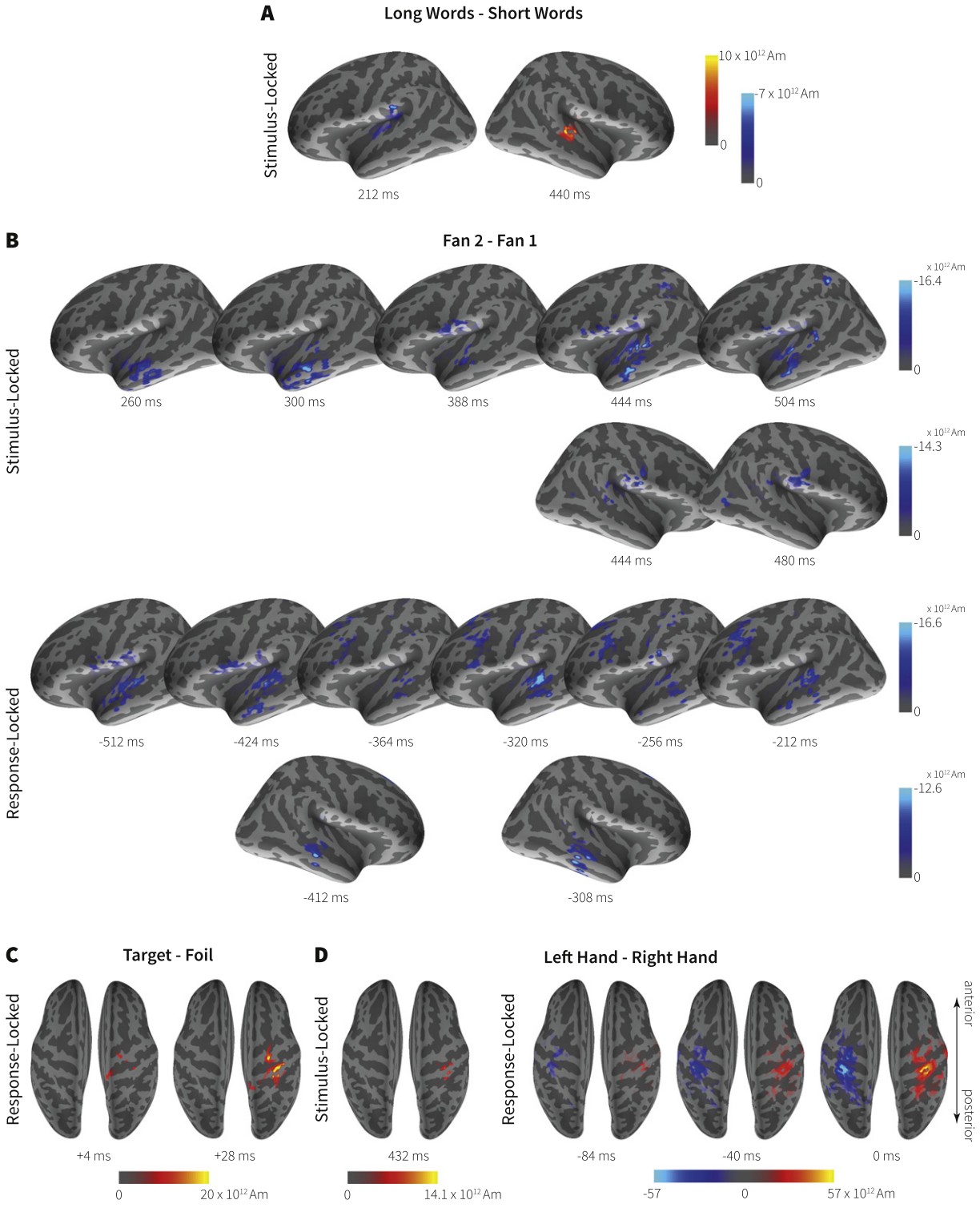

Fig. 4. Difference in source estimates for long–short words (A), fan 2–fan 1 pairs (B), target–foils (C), and left–right-handed responses (D).

possible frequency per block – when no errors were made – is 1 because each target word was presented at least once per block. Block 1–3 indicate the blocks during the training phase on the first day of the experiment, Block 4 indicates the additional block of cued recall just before the test phase in the scanner. A repeated-measures ANOVA indicated that frequency decreased over blocks, as reflected by a main effect of Block ($F(3,51) = 61.02$, $p < 0.001$, $\eta_p^2 = 0.78$), and was lower for Fan 1 items than for fan 2 items ($F(1,17) = 48.21$, $p < 0.001$, $\eta_p^2 = 0.74$). The effect of fan decreased over blocks, as indicated by a significant interaction between block and fan ($F(3,51) = 39.79$, $p < 0.001$, $\eta_p^2 = 0.70$). There were no other effects (all Fs < 1).

Test phase

The middle panel of Fig. 3 shows RTs during the test phase, the right panel error rate. RT was longer and error rate was higher for fan 2 items compared to fan 1 items (RT: $F(1,17) = 67.43$, $p < 0.001$, $\eta_p^2 = 0.80$; Error rate: $F(1,17) = 27.38$, $p < 0.001$, $\eta_p^2 = 0.62$), and for Foils compared to Targets (RT: $F(1,17) = 62.94$, $p < 0.001$, $\eta_p^2 = 0.79$; Error rate

Table 1
Properties of significant clusters.

Location	Coordinates	Time	Size (max)	Source contrast ($\times 10^{-12}$)	p-Value
Long words–short words (stimulus-locked)					
L supra marginal, transverse temporal	−44, −29, 12	176–256	18.76 (43)	−1.79	0.014
R superior temporal	55, −27, 4	408–484	14.45 (31)	2.98	0.030
Fan 2–fan 1 (stimulus-locked)					
L insula, superior temporal, middle temporal, supra marginal, precentral, transverse temporal, parahippocampal, postcentral, inferior temporal, entorhinal, pars opercularis, banks of the STS	−49, −15, −5	220–604	73.73 (188)	−3.86	<0.001
L superior parietal, paracentral	−31, −45, 51	332–544	11.72 (39)	−3.56	0.018
R banks of the STS, supra marginal, postcentral, superior temporal, inferior parietal	50, −35, 13	368–636	24.85 (56)	−2.97	0.002
L isthmus cingulate	−7, −37, 27	412–756	5.92 (21)	−0.373	0.031
Fan 2–fan 1 (response-locked)					
L superior temporal, insula, middle temporal, transverse temporal, supra marginal, postcentral, banks of the STS, precentral	−54, −22, −1	−648 to −116	44.58 (147)	−4.28	<0.001
L superior frontal, posterior cingulate, caudal middle frontal, caudal anterior cingulate, postcentral, paracentral, precentral, rostral middle frontal, ishtmus cingulate, pars opercularis, supra marginal	−28, 6, 40	−512 to −152	47.41 (122)	−2.66	<0.001
R middle temporal, superior temporal, supra marginal, inferior temporal	51, −30, −9	−460 to −216	17.84 (47)	−3.63	0.008
Target–foil (response-locked)					
R precentral, postcentral	29, −28, 59	−20–+88	22.79 (55)	7.64	0.007
Left hand–right hand (stimulus-locked)					
R postcentral	39, −27, 52	284–576	4.35 (15)	5.27	0.045
Left hand–right hand (response-locked)					
R postcentral, precentral, superior parietal, supra marginal, inferior parietal, caudal middle frontal	37, −31, 52	−160–+104	76.10 (187)	15.0	<0.001
R postcentral, insula, precentral, supra marginal, superior temporal, banks of the STS, transverse temporal	54, −14, 22	−148–+92	46.75 (119)	7.85	0.002
L postcentral, precentral, superior parietal, supra marginal, caudal middle frontal, precuneus	−35, −31, 55	−164–+148	76.77 (209)	−15.3	<0.001
R temporal pole, fusiform, superior temporal	34, −1, −27	−144–+96	26.95 (80)	−6.81	0.006
L postcentral, supra marginal, insula, superior temporal, precentral, transverse temporal	−54, −22, 24	−116–+112	56.38 (127)	−8.17	0.002

Note: Location lists ROIs with 100 or more sources in the cluster, in order of contribution; L/R indicates hemisphere. Coordinates indicate center-of-mass of current estimates in MNI coordinates. Time is time in ms since stimulus, before response (−) or after response (+). Size indicates mean size over time; max size indicates maximum size. Source contrast indicates difference in mean estimated current in Am. p-Value indicates the permutation cluster p-value.

marginally significant: $F(1,17) = 3.56$, $p = 0.077$, $\eta_p^2 = 0.17$). In addition, the effect of fan on RT was larger for foils than for targets, as indicated by a significant interaction between fan and Probe type ($F(1,17) = 8.79$, $p = 0.009$, $\eta_p^2 = 0.34$). These results indicate that foils were slightly more difficult to identify than targets, and that fan 2 items were more difficult than fan 1 items. Neither word length nor response hand had a significant effect on behavior. All behavioral effects are in line with previous associative recognition studies (e.g., Anderson and Reder, 1999; Borst et al., 2013; Schneider and Anderson, 2012).

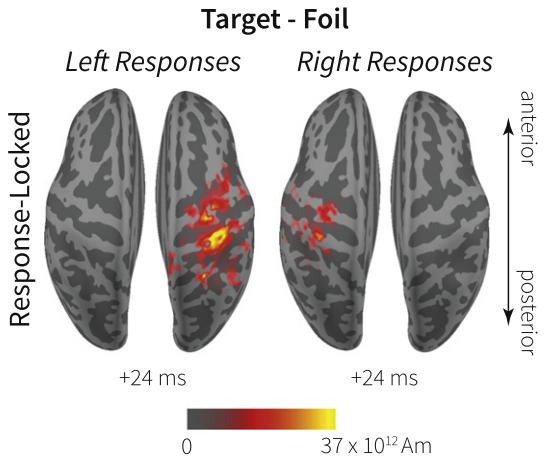

Fig. 5. Difference in source estimates for target–foils, separately for left-handed and right-handed responses.

MEG source estimates

For the source estimates we performed non-parametric cluster-based permutation tests to control for multiple comparisons (Maris and Oostenveld, 2007). We report clusters with a permutation p-value < 0.05; Fig. 4 shows contrasts between source estimates of two conditions (e.g., left-handed–right-handed responses) for sources in significant clusters. In addition, we included the full 4D t-maps and source estimates (both raw and thresholded based on the identified clusters) as Supplementary Material. Table 1 reports the clusters for all contrasts; location names are based on the ROIs in the Desikan-Killiany atlas (Desikan et al., 2006).

Word length

Fig. 4A shows stimulus-locked contrasts between long and short words (positive values indicate that long words resulted in higher source estimates, negative values that short words resulted in higher source estimates). Two clusters were identified: one cluster between 176 and 256 ms and one cluster between 408 and 484 ms (Table 1). In the early cluster, short words resulted in higher currents around the posterior part of the superior temporal lobe in the left hemisphere. In the later cluster, long words caused higher current than short words in a similar area in the right hemisphere. The response-locked analysis did not yield any significant clusters.

Associative fan

Fig. 4B shows stimulus-locked (top) and response-locked (bottom) effects of the fan manipulation. In all clusters, fan 1 pairs resulted in greater estimated currents than fan 2 pairs. The combination of the stimulus-locked and response-locked analyses shows that the first

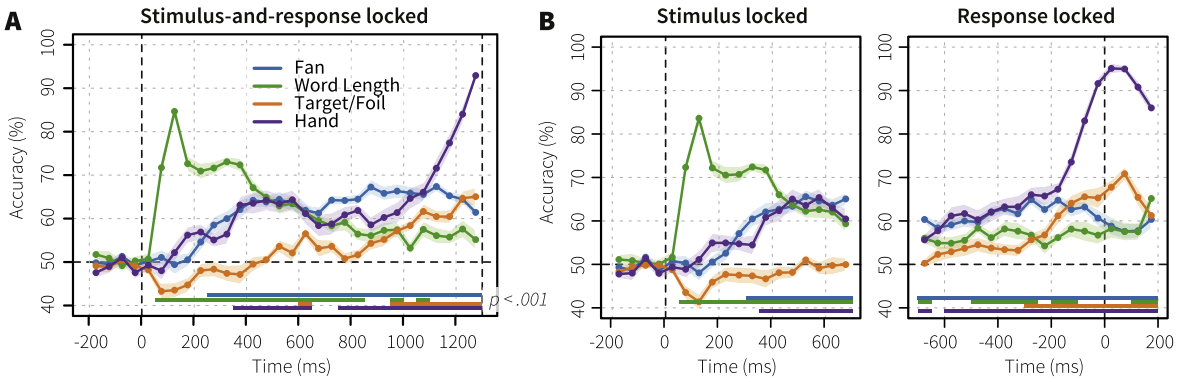

Fig. 6. Results of the sensor-based classifier: A) stimulus-and-response-locked results, B) stimulus locked and response-locked results separately. Horizontal lines at the bottom of the graphs indicate where classification accuracy was significantly ($p < 0.001$) different from chance (50%) across subjects.

differences (220–350 ms) occurred in the lower parts of the middle and superior temporal ROIs. Activity then moves forward and upward to the lower parts of the post- and precentral gyri and the supramarginal ROI (370–640 ms). From about 350 ms before the response (~950 ms post-stimulus) we also see prefrontal activity, focused around the superior frontal and caudal middle frontal ROIs. This latter area overlaps with the area that ACT-R links to declarative memory retrievals (Anderson, 2007; Borst et al., 2015), and is consistently implicated in fMRI studies of the fan effect (e.g., Danker et al., 2008; Sohn et al., 2003, 2005). The early effects occurred in both hemispheres, but were stronger in the left hemisphere; the prefrontal effect was absent from the right hemisphere.

Probe type

Differences between targets and foils became apparent very late in the associative recognition trials. The only significant cluster was found in the response-locked analysis, from 20 ms before the response until 88 ms after the response, in the right pre- and postcentral ROIs. Fig. 4C and D indicate that this cluster essentially overlaps with the left-handed motor cluster we see in the response-hand analysis.

To check whether this cluster reflects differences in motor activity (i.e. between index finger for targets and middle finger for foils) instead of activity related to memory representation or decision making, as we intended, we performed an additional response-locked analysis. In this analysis we looked at effects of probe type separately for left- and right-handed response blocks. Fig. 5 shows the results. For left-handed responses we found the same cluster as in the overall analysis (−16–88 ms; permutation p-value < 0.001; cf. Fig. 4C). For right-handed responses we did not find this cluster, instead we identified a cluster in the left hemisphere with similar timing and location as the cluster for left-handed responses (−48–52 ms; permutation p-value = 0.007). This suggests that the probe type cluster in Fig. 4C reflects a difference between motor processing for index fingers and middle fingers (with index fingers yielding the stronger signal), instead of a processing difference between targets and foils. Apparently this difference is stronger for left-handed responses than for right-handed responses, as we only identified the right-hemispheric cluster in the overall analysis (also evident in Fig. 5).

Response hand

As expected, left-handed responses resulted in higher estimates than right-handed responses in the right motor cortex, and right-handed responses in higher estimates in the left motor cortex. These clusters started around 150 ms before the response and extended into the post-response interval.

Table 2
Classification accuracy in ROIs.

Location	% correct	p-Value	Location	% correct	p-Value
Word length			**Probe type**		
L lateral occipital	79.84	<0.001	L precuneus	53.31	0.08
R lateral occipital	76.89	<0.001	L superior parietal	52.83	0.08
R lingual	75.01	<0.001	L precentral	52.25	0.18
L pericalcarine	74.44	<0.001	R entorhinal	51.75	0.12
L lingual	73.76	<0.001	L paracentral	51.65	0.22
R pericalcarine	73.02	<0.001	L caudal anterior cingulate	51.43	0.16
L cuneus	70.44	<0.001	L fusiform	50.92	0.33
R cuneus	69.50	<0.001	R insula	50.70	0.35
L fusiform	68.06	<0.001	L supramarginal	50.70	0.33
R fusiform	66.64	<0.001	L postcentral	50.61	0.39
Fan			**Response hand**		
R lingual	61.98	<0.001	L&R precentral	76.10	<0.001
L inferior parietal	61.94	<0.001	R postcentral	73.90	<0.001
L lingual	61.90	<0.001	L postcentral	73.71	<0.001
L lateral occipital	61.68	<0.001	L precentral	71.96	<0.001
L insula	61.56	<0.001	R precentral	68.29	<0.001
L middle temporal	61.04	<0.001	R superior parietal	66.90	<0.001
L fusiform	60.82	<0.001	L superior parietal	66.36	<0.001
L superior temporal	60.47	<0.001	R supramarginal	66.08	<0.001
L postcentral	60.25	<0.001	R paracentral	63.56	<0.001
L superior parietal	60.07	<0.001	L paracentral	63.55	<0.001

Note: L and R indicate left and right hemisphere, respectively. L&R indicates an ROI defined over both hemispheres.

Classifier

Although the permutation analysis identifies significant clusters, it is a univariate analysis in the sense that single sources have to show a significant effect before they are taken into account. In contrast, the classifier combines information from multiple sources and time points to distinguish different conditions, potentially making the analysis more sensitive.

Time

To determine when information related to the experimental conditions was processed, we applied the classifier to the MEG sensor data. First, we investigated if the classifier could reliably estimate to which condition an example belonged using the full interval (i.e. 200 ms before the stimulus until the response). For Word Length, the classifier determined the correct condition in 83.8% of the examples, far above the 50% chance level. Likewise, fan (79.8%), Probe Type (65.9%), and Response Hand (88.3%) also could be classified reliably, but note that Probe Type was considerably harder to classify than the other conditions. As the second step, we divided the sensor data into 50-ms intervals and applied the classifier to these intervals separately. Fig. 6A shows the results for the stimulus-and-response locked data, Fig. 6B for the stimulus-locked and response-locked data separately.

Word Length was the first condition to be classified correctly, starting in the 50–100 ms interval. It peaks between 100 and 150 ms, stays elevated until 400 ms, then slowly decreases, but can be classified quite reliably up to the end of the trial. The second condition to be classified correctly was associative fan, from 250 ms onwards. Third is response hand (recall that target and foils required different fingers of the same hand, not a different hand), starting at 350 ms but clearly peaking at the end of the trial. Finally, probe type could be reliably classified from about 300 ms before the response.

Location

Knowing when the conditions could be identified in the MEG signal is a first step in determining the processing stages participants moved through to perform the associative recognition task. To further investigate the content of the processing stages, we applied the classifier to the 68 ROIs of the Desikan-Killiany atlas. For Response Hand we defined an additional region of interest: the combination of the precentral ROIs of both hemispheres, as this should most clearly account for hand. First, we used the full interval from 200 ms before the stimulus until the response, to determine ROIs of interest. For ROIs in which we could classify a condition reliably, we divided the data in 50-ms intervals to see at what times the ROI was involved in processing. Table 2 lists the top 10 ROIs with the highest classification accuracy for each condition; Fig. 7 shows classification accuracy for significant ROIs ($p < 0.001$ across subjects) and classification over time for a selection of these ROIs. Supplementary Table 1 lists classification accuracy of all ROIs for each condition (i.e. it is a complete version of Table 2).

Unlike the standard analysis, the classifier clearly identified the lateral occipital ROIs as the main regions involved in Word Length effects, especially between 50 and 150 ms. Confirming the standard analysis, fan could best be classified in temporal, inferior parietal, and prefrontal ROIs, including the insula (Fig. 7B). None of the ROIs contained sufficient information to classify Probe Type consistently across subjects. Finally, as expected, Response Hand could best be classified by the combination of the precentral ROIs of both hemispheres – classification accuracy rising sharply towards the end of the trial (Fig. 7C).

General discussion

The goal of this study was to get more insight in the cognitive processes underlying associative recognition, and thereby evaluate associative recognition theories. In particular, we aimed to identify the number, nature, timing, and location of memory processes involved in associative recognition. To track cognitive processes both in time and space we applied MEG: its millisecond resolution provides more information on the timing of these processes than the aggregate measures of fMRI or behavior, while its reasonable spatial resolution yields more information on the content of these processes than the coarse localization of EEG measurements. In this final section we discuss the detailed spatio-temporal model of associative recognition that resulted.

In the experiment, we manipulated word length, associative fan, probe type, and response hand, which were each intended to tap one of the proposed cognitive processes: perceptual encoding, associative retrieval, decision making, and response generation, respectively. By tracking the effects of these manipulations with univariate cluster-based permutation tests, as well as with a multi-variate classifier, we aimed to get more insight in the nature and timing of the underlying processes. The general picture that arose was a posterior-to-prefrontral progression of activity during the first 1100 ms of each trial, after which the activity moved to parietal and motor cortices to issue the response at around 1300 ms (Figs. 4 and 7). The earliest effects are related to word length – and by association perceptual encoding – starting at 50 ms in the lateral occipital cortex. Second, associative fan showed effects from 220 ms onwards, indicating memory processing. Finally, the probe type and response hand manipulations resulted in effects starting around 300 ms before the response. We will now discuss these results in detail, followed by the implications for theories of associative recognition. The results are summarized in Fig. 8, showing the timing and location of the inferred cognitive processes in associative recognition.

Processing stages

Word length: perceptual encoding

As expected, Word Length did not affect response time (Juhasz and Rayner, 2003; Spinelli et al., 2005). It did result in the earliest effects on the MEG signal, however, leading to successful classification starting in the 50-ms interval and continuing up to the end of the trial (Figs. 6 and 7). Classification accuracy was highest in right and left lateral occipital regions. This is in line with earlier studies, both standard EEG/MEG analyses (Assadollahi and Pulvermüller, 2003; Hauk et al., 2006; Hauk and Pulvermüller, 2004) and classification approaches (Borst et al., 2013; Sudre et al., 2012). Although this early occipital effect did not survive the cluster analysis (Fig. 4A), we do find this effect clearly between 60 and 140 ms when looking at a univariate contrast *without* correcting for multiple comparisons (Fig. 8, top left). Classification accuracy stays high until 400 ms, after which long and short words are harder to distinguish – although classification is still possible. The cluster analysis confirmed word length effects up to 480 ms, with the effects between 180 and 480 ms being located in dorsal temporal regions, on the border with the supramarginal gyrus. Similar effects were reported in several studies (e.g., Borst et al., 2013; Hauk et al., 2006; Hauk et al., 2009; Hauk and Pulvermüller, 2004).

If we assume that word length effects indicate perceptual encoding, we can conclude that encoding starts at 60 ms, or perhaps a little earlier if word length (i.e. the total size of the stimulus) is not the first information to register. The words are processed between 60 and 140 ms in visual occipital regions, in which the signal is known to be modulated by word length, and where the effect probably reflects the more extended visual stimuli rather than differences in lexical access (Assadollahi and Pulvermüller, 2003; Hauk and Pulvermüller, 2004; Indefrey et al., 1997). Afterwards, the activity moves to dorsal temporal regions, which are thought to be involved in lexical and semantic processing (Assadollahi and Pulvermüller, 2003; Hauk et al., 2006, 2009). If we assume that the temporal activity indicates access to the identity of the words and their meaning, we can conclude that from 180 ms onwards general memory processes can begin to identify whether these

words – and their combination – were encountered during the training phase of the experiment. Finally, word length can be classified above chance until the end of the trial, which might be due to the continuing visual input.

Associative fan: memory retrieval

The associative fan manipulation resulted in activity that can be divided into three patterns, with fan 1 items always resulting in greater estimated currents than fan 2 items. First, the cluster analysis showed an effect from 220 to 350 ms in the lower parts of the middle and superior temporal regions. This pattern extended up to about 100 ms before the response (Table 1). Second, from 370 ms after the stimulus till about 400 ms before the response, we found activity in the supramarginal ROI and the lower parts of the post- and precentral gyri. The classifier located this effect in the left inferior parietal ROI, starting at 400 ms (Fig. 7). Third, from about 350 ms before the response (~950 ms post-stimulus), fan 1 items resulted in greater activity in the prefrontal cortex, the left caudal middle frontal ROI. This area is consistently implicated in fMRI studies of the fan effect (e.g., Danker et al., 2008; Sohn et al., 2005, 2003).

In the previous section we hypothesized that lexical access starts around 180 ms into the trial. From that point onwards we might also expect to find differences between fan 1 and fan 2 words, as fan 2 words were encountered more often than fan 1 words (fan 2 *words* were presented more frequently during training, left panel of Fig. 3, and occurred in two pairs). We hypothesize that this is reflected in the first of the three distinguishable fan processes, and constitutes the familiarity process in dual-process models (e.g., Rugg and Curran, 2007; Yonelinas, 2002). Whereas the timing overlaps with the FN400 effect of EEG data (300–500 ms), its location is different: in EEG data a negativity over mid-frontal electrodes is associated with this effect, while in our data it is a clear temporal effect. Supporting our interpretation, Gonsalves and colleagues have shown that medial temporal cortex activity correlates with stimulus familiarity between 150 and 300 ms post-stimulus in MEG recordings (Gonsalves et al., 2005). Furthermore, fMRI and lesion studies have shown that familiarity is dependent on structures in the medial temporal lobe, most strongly on the perirhinal cortex (Diana et al., 2007; Henson, 2005; Rugg and Yonelinas, 2003), making source projections of this effect on the superior and middle temporal lobes reasonable. This interpretation matches our earlier EEG findings, where we contrasted new foils (entirely new distractor pairs) with re-paired foils to isolate a familiarity process, resulting in a difference between 180 and 380 ms (Borst and Anderson, 2015a). Although the activity in this region continues almost until the end of the trial, we assume that the actual familiarity process is early, between 180 and 380 ms, based on the EEG evidence and the literature. The continued difference in activity might be due to accessing information to support recollection and representational processes.

We hypothesize that the second process reflects recollection of the associative information. We assume that the activity projected onto the supramarginal ROI, the lower parts of the post- and precentral gyri, and the superior temporal ROI, originates in the hippocampus and surrounding areas, which are known to be instrumental in recollection (e.g., Bunge et al., 2004; Diana et al., 2007; Henson, 2005; Rugg and Yonelinas, 2003; Stark and Squire, 2001). Furthermore, the timing of the process (370–900 ms) overlaps with the recollection process assumed by dual-process theories (parietal old/new effect, 500–800 ms), and also matches the recollection process and associated working memory process identified in our EEG data (~250–750 ms; Borst and Anderson, 2015a). Finally, it has been shown that activating the temporal cortex with transcranial direct current stimulation improves recognition of old items, possibly by boosting recollection (Pisoni et al., 2015).

The area of the third pattern, in the prefrontal cortex, is in fMRI studies of associative recognition often linked to declarative memory retrieval, or recollection (Anderson, 2007; Borst and Anderson, 2013; Danker et al., 2008; Lepage et al., 2003; Sohn et al., 2005). However, the high temporal resolution of MEG revealed that this is a late effect, starting at 950 ms post-stimulus. Combined with the interpretation of the other processes, we hypothesize that the activity in this area reflects the maintenance of the recollected information while the decision is made, instead of the recollection process itself. This is in line with research that implies that this region is involved in post-retrieval monitoring, also for associative information (e.g., Achim and Lepage, 2005; Mitchell et al., 2004; Rugg et al., 2003). Likewise, Ghuman et al. (2008) proposed that this prefrontal area is used as a mapping between recollection and decision in a priming study. Anderson et al. (2016) found evidence for such a representation process in associative recognition, of which the activation strength depended on the strength of the memories – here the difference between fan 1 and fan 2 pairs (note that they proposed a parietal representation, however, based on EEG). Borst and Anderson (2015a) posited a decision process between 700 and 1000 ms, which could act upon the information that is represented in this area.

Although we divided the fan activity into three patterns for ease of discussion, especially the first two patterns seem highly related and overlapping. It has also been argued that there is no clear regional distinction in the medial temporal lobe between familiarity and recollection processes, although familiarity manipulations seem to result in stronger effects in the perirhinal cortex and recollection manipulations in stronger effects in the hippocampus (e.g., Diana et al., 2007; Henson, 2005). That said, at the very least we observed an increase in the total activation in these regions starting at 370 ms, implying that recollection is taking place – also based on the timing of the increased activation (unfortunately, we did not include an independent familiarity manipulation in the current experiment). For this reason, combined with previous evidence (Borst and Anderson, 2015a), we hypothesize that the familiarity process itself ends around this time. The continued activity might signify access in support of the recollection process. The third pattern of activity, in the prefrontal cortex was more clearly separated from the other clusters. To better distinguish different processing stages, future studies could do an item-level representational similarity analysis (RSA) to examine the transition from visually oriented similarity between true pairings and foil stimuli to semantically oriented similarity, as suggested by one of our reviewers.

Interestingly, all of the effects were in the direction of greater activity for lower fan items (in line with previous EEG studies, e.g., Borst et al., 2013). This contrasts with fMRI, where higher fan items yield greater activity than lower fan items (Danker et al., 2008; Khader et al., 2007; Sohn et al., 2005). We believe this is due to the sluggishness of the fMRI BOLD response. Fan 1 items do elicit greater activity, but for a shorter duration than fan 2 items (i.e. RTs are longer for fan 2 items). The longer duration of fan 2 items results in a higher BOLD response over the whole trial, but not in greater M/EEG activity at any one point in time.

Probe type: decision

The effect of probe type was intended to indicate a decision process. Surprisingly – given that the task was to distinguish targets and re-paired foils, and we are looking at correct trials – the cluster analysis only identified a very late cluster starting 20 ms before the response and lasting until 90 ms after the response (Table 1). Furthermore, this cluster was located over the right motor cortex and not over areas traditionally implicated in decision making (Fig. 4). A follow-up analysis that separated left- and right-handed responses suggested that this cluster is related to differences in motor processing between index finger (targets) and middle finger (foils), as it only shows up for left-handed responses, and a similar cluster in the left hemisphere was identified

Fig. 7. Results of the source-based classifier. Colors in the surface plots indicate classification accuracy of the ROI when using the full interval from stimulus till response for ROIs that resulted in significant above-chance classification across subjects; line plots show classification accuracy over time for a particular ROI.

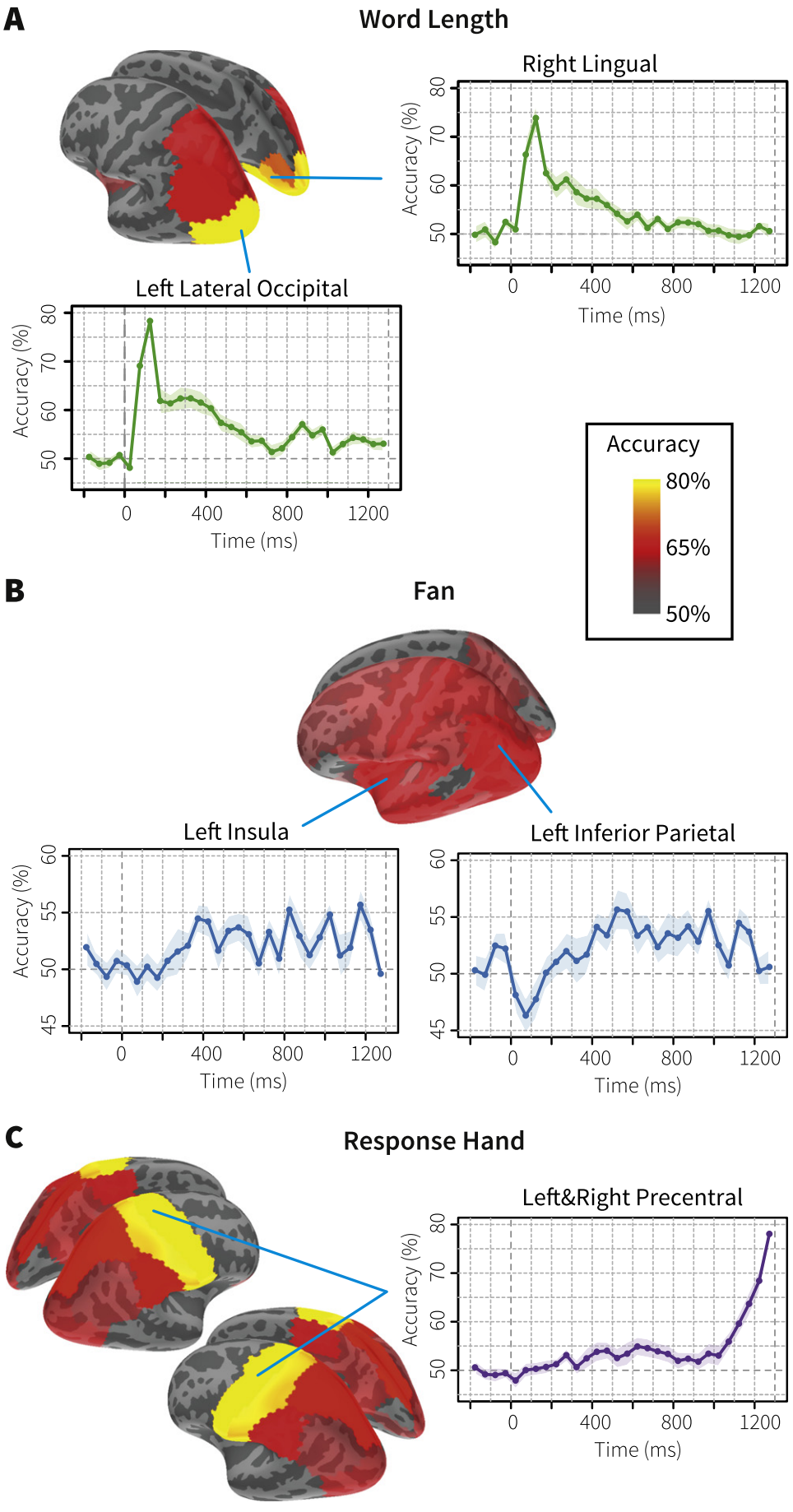
A
Word Length
Right Lingual
Left Lateral Occipital
Accuracy (%)
Time (ms)
Accuracy
80%
65%
50%
B
Fan
Left Insula
Left Inferior Parietal
C
Response Hand
Left&Right Precentral

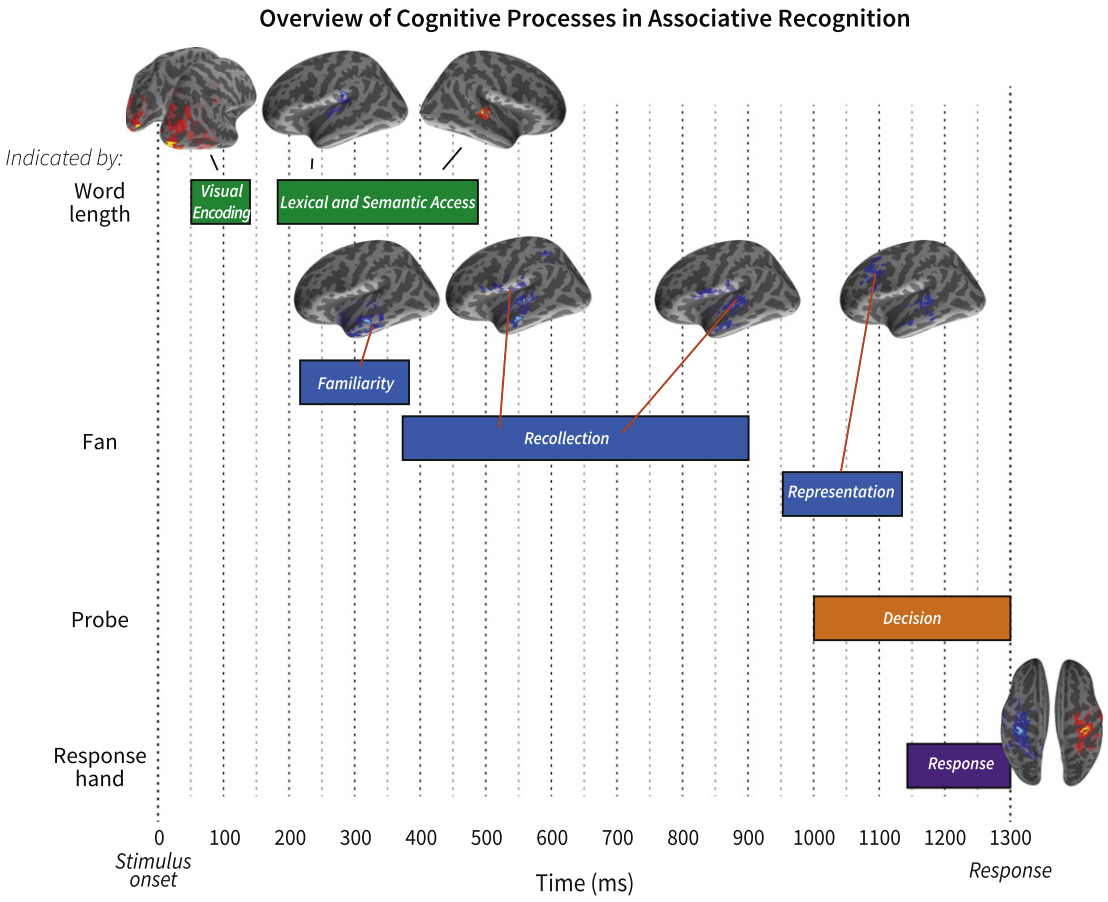

Fig. 8. Overview of the cognitive processes in associative recognition as indicated by the current results in combination with the previous literature. See the main text for details.

for right-handed responses (Fig. 5). It is conceivable that the index finger is represented stronger in the brain, and therefore causes a sharper peak of activity than middle-finger responses (it is plausible that differences between fingers can be measured with MEG, see e.g., Beisteiner et al., 2004; Hadoush et al., 2011; Inoue et al., 2013). We only found the effect over right motor cortex in the overall analysis, perhaps because the difference between index and middle finger is greater for the left hand for our right-handed participants.

The multivariate classifier turned out to have more power, and resulted in reliable classification starting 300 ms pre-response (Fig. 6B), whereas the motor effects identified by the cluster analysis started at 45 ms pre-response. Although this was also partly based on the precentral motor ROI, the left precuneus and left superior parietal contributed to classification (Table 2, Fig. 7). These regions might indicate an actual decision process, which would match a central-parietal effect in the EEG study that was characterized by a more positive signal for targets compared to re-paired foils between 350 and 50 ms before the response (Borst et al., 2013). It also resembles the parietal old/new effect (e.g., Rugg and Curran, 2007), although that is typically measured by comparing old and completely new items, while in our experiment only the associative status of the pair is new, and not the individual words (see also Speer and Curran, 2007, who showed a parietal old/new effect in response to associative status).

It is possible that the decision process itself is very similar between targets and re-paired foils – just the outcome is different – and that it is therefore hard to find activity due to this process.[5] All models discussed in the introduction propose a recall-to-reject process for re-paired foils, which means that in our experiment highly similar information is retrieved for targets and re-paired foils (a word pair). This would not result in a different activation pattern. The decision process then compares the recollected information that is represented in the prefrontal cortex (the third fan pattern above) to the information on the screen. This should also result in similar activation patterns, except for the final decision. We hypothesize that this is indeed the case, and that it is the reason for finding so few differences in activity between targets and re-paired foils, even though participants made the right decisions and performed very well.

Response hand: response

Finally, response hand was varied between blocks and should indicate a response process. The cluster analysis showed a very early cluster 280 ms after stimulus onset in the right hemisphere, and both a left and a right cluster starting about 160 ms before the response. All results were over the left and right motor cortices. The classifier yielded similar results, with successful classification starting around 400 ms (Fig. 6), but with a sharp peak in the last 150 ms before the response. These results imply that participants were anticipating giving a response already early on in the trial (note that this analysis compares blocks, not targets and foils, and that such an effect is therefore reasonable as response hand was varied between blocks), but that motor programming of the finger press itself took place in the last 160 ms before the response.

A spatio-temporal model of associative recognition

Fig. 8 gives an overview of the cognitive processes in associative recognition that were identified in the current study, and that form the basis for a detailed spatio-temporal model of associative recognition. As became clear, three memory processes play a role: familiarity, recollection, and representation. Familiarity and recollection were localized

[5] Although there are clear differences in reaction times and accuracy between targets and foils, we argue these are due to the memory processes, not to the decision process itself.

to structures in the medial temporal lobe and the supramarginal gyrus, and the recollected information was represented in the prefrontal cortex. This indicates that, at least for associative recognition, neither single-process theories (e.g., Gillund and Shiffrin, 1984; Wixted, 2007) nor the original ACT-R model (Fig. 1, top) can explain the data. Dual-process theories and the EEG model (Fig. 1, bottom) give a better account of these processes: we found evidence for an early familiarity process followed by recollection. However, also these theories did not include a separate representation process.

The original ACT-R model (Fig. 1, top) was based on behavior and fMRI data, and did not include a familiarity process. Where the EEG data already gave indications for a separate familiarity process (Borst and Anderson, 2015a), the superior localization of MEG adds a representational process in the prefrontal cortex to the model. This region had been implicated in imaging studies of associative recognition as the region responsible for recollection (e.g., Sohn et al., 2003). As the superior temporal resolution of MEG showed, this region only became active relatively late in the process, implying that it is used to store the results of a recollection process instead of for recollection itself. The EEG data also indicated a relatively complex decision process (Fig. 1, bottom). The current MEG results help to understand this process: it indicated that the actual decision process might be located in the parietal cortex, and acts upon information represented in the prefrontal cortex by comparing it to the word pair encoded from the screen. This is close to the fMRI-informed ACT-R model (e.g., Sohn et al., 2005), which assumes a 200 ms representational process followed by a brief (50 ms) decision.

Conclusions

By using non-parametric cluster analyses of MEG source estimates, and training a machine-learning classifier both on MEG sensor data as well as source estimates in 68 regions of interest, we were able to sketch a relatively detailed model of associative recognition both in time and space (Fig. 8). This model indicates where existing theories have to be adapted: besides a familiarity stage (single-process models) and a recollection stage (dual-process models, ACT-R), there also needs to be a representation stage, during which a decision process acts upon the recollected information.

In addition to yielding new information on associative recognition, this study also highlights the limits of behavioral data and fMRI data. We have argued before that behavioral data is insufficient to constrain models of cognition (Borst et al., 2015; Nijboer et al., 2016) as it only indicates the cumulative duration of all processes (see also Anderson et al., 2016). fMRI helps by attributing different processes to different brain regions, in effect splitting a single process in to multiple processes in space. Similarly, EEG helps dividing the cumulative process into smaller temporal episodes, which for instance helped to identify the familiarity process (Borst and Anderson, 2015a). MEG provided key additional information by allowing for an analysis in both time and space. For instance, although fMRI had identified the importance of the prefrontal region, because of fMRI's low temporal resolution it was unclear that this region only becomes active relatively late in a task, and can therefore not represent the recollection process itself.

To analyze the MEG data, we used non-parametric cluster-based permutation tests (Maris and Oostenveld, 2007) and a multivariate classifier. The classifier turned out to be more powerful than the cluster-based analyses, and for instance identified an early visual effect (which was also observable in the data when not correcting for multiple comparisons). This illustrates the power of such a classifier, which can identify processes that are either only present when combining activity from multiple sources, or where multiple-comparison corrections limit the power of a mass-univariate analysis. On the other hand, activity patterns on which the decisions of a classifier are based are often hard to interpret, so we recommend using a classifier in combination with more standard univariate analyses.

Supplementary data to this article can be found online at http://dx.doi.org/10.1016/j.neuroimage.2016.08.002.

Acknowledgements

This research was supported by a James S. McDonnell Foundation (220020162) Scholar Award to John Anderson and an NWO Veni grant (451-15-040) awarded to Jelmer Borst.

References

Achim, A.M., Lepage, M., 2005. Dorsolateral prefrontal cortex involvement in memory post-retrieval monitoring revealed in both item and associative recognition tests. NeuroImage 24 (4), 1113–1121. http://dx.doi.org/10.1016/j.neuroimage.2004.10.036.
Anderson, J.R., 1983. The Architecture of Cognition. Harvard University Press, Cambridge, MA.
Anderson, J.R., 2007. How Can the Human Mind Occur in the Physical Universe? Oxford University Press, New York
Anderson, J.R., Bower, G.H., 1973. Human Associative Memory. Holt, Rinehart & Winston, New York.
Anderson, J.R., Reder, L.M., 1999. The fan effect: new results and new theories. J. Exp. Psychol. Gen. 128 (2), 186–197. http://dx.doi.org/10.1037/0096-3445.128.2.186.
Anderson, J.R., Carter, C.S., Fincham, J.M., Qin, Y., Ravizza, S.M., Rosenberg-Lee, M., 2008. Using fMRI to test models of complex cognition. Cogn. Sci. 32, 1323–1348.
Anderson, J.R., Zhang, Q., Borst, J.P., Walsh, M.M., 2016. The Discovery of Processing Stages: Extension of Sternberg's Method Psychological Review.
Assadollahi, R., Pulvermüller, F., 2003. Early influences of word length and frequency: a group study using MEG. Neuroreport 14 (8), 1183–1187. http://dx.doi.org/10.1097/01.wnr.0000075305.76650.60.
Beisteiner, R., Gartus, A., Erdler, M., Mayer, D., Lanzenberger, R., Deecke, L., 2004. Magnetoencephalography indicates finger motor somatotopy. Eur. J. Neurosci. 19 (2), 465–472. http://dx.doi.org/10.1111/j.1460-9568.2004.03115.x.
Borst, J.P., Anderson, J.R., 2013. Using model-based functional MRI to locate working memory updates and declarative memory retrievals in the fronto-parietal network. Proc. Natl. Acad. Sci. U. S. A. 110 (5), 1628–1633. http://dx.doi.org/10.1073/pnas.1221572110.
Borst, J.P., Anderson, J.R., 2015a. The discovery of processing stages: analyzing EEG data with hidden semi-Markov models. NeuroImage 108, 60–73.
Borst, J.P., Anderson, J.R., 2015b. Using the cognitive architecture ACT-R in combination with fMRI data. In: Forstmann, B.U., Wagenmakers, E.-J. (Eds.), Model-based Cognitive Neuroscience. Springer, New York.
Borst, J.P., Schneider, D.W., Walsh, M.M., Anderson, J.R., 2013. Stages of processing in associative recognition: evidence from behavior, electroencephalography, and classification. J. Cogn. Neurosci. 25 (12), 2151–2166.
Borst, J.P., Nijboer, M., Taatgen, N.A., Van Rijn, H., Anderson, J.R., 2015. Using data-driven model-brain mappings to constrain formal models of cognition. PLoS One 10 (3), e0119673. http://dx.doi.org/10.1371/journal.pone.0119673.
Bunge, S.A., Burrows, B., Wagner, A.D., 2004. Prefrontal and hippocampal contributions to visual associative recognition: interactions between cognitive control and episodic retrieval. Brain Cogn. 56 (2), 141–152. http://dx.doi.org/10.1016/j.bandc.2003.08.001.
Chan, A.M., Halgren, E., Marinkovic, K., Cash, S.S., 2011. Decoding word and category-specific spatiotemporal representations from MEG and EEG. NeuroImage 54 (4), 3028–3039. http://dx.doi.org/10.1016/j.neuroimage.2010.10.073.
Coltheart, M., 1981. The MRC psycholinguistic database. Q. J. Exp. Psychol. 33A, 497–505.
Dale, A.M., Fischl, B., Sereno, M.I., 1999. Cortical surface-based analysis. I. Segmentation and surface reconstruction. NeuroImage 9 (2), 179–194. http://dx.doi.org/10.1006/nimg.1998.0395.
Danker, J.F., Gunn, P., Anderson, J.R., 2008. A rational account of memory predicts left prefrontal activation during controlled retrieval. Cereb. Cortex 18 (11), 2674–2685. http://dx.doi.org/10.1093/cercor/bhn027.
Das, K., Giesbrecht, B., Eckstein, M.P., 2010. Predicting variations of perceptual performance across individuals from neural activity using pattern classifiers. NeuroImage 51 (4), 1425–1437. http://dx.doi.org/10.1016/j.neuroimage.2010.03.030.
Delorme, A., Makeig, S., 2004. EEGLAB: an open source toolbox for analysis of single-trial EEG dynamics including independent component analysis. J. Neurosci. Methods 134 (1), 9–21. http://dx.doi.org/10.1016/j.jneumeth.2003.10.009.
Desikan, R.S., Segonne, F., Fischl, B., Quinn, B.T., Dickerson, B.C., Blacker, D., ... Killiany, R.J., 2006. An automated labeling system for subdividing the human cerebral cortex on MRI scans into gyral based regions of interest. NeuroImage 31 (3), 968–980. http://dx.doi.org/10.1016/j.neuroimage.2006.01.021.
Diana, R.A., Reder, L.M., Arndt, J., Park, H., 2006. Models of recognition: a review of arguments in favor of a dual-process account. Psychon. Bull. Rev. 13 (1), 1–21. http://dx.doi.org/10.3758/BF03193807.
Diana, R.A., Yonelinas, A.P., Ranganath, C., 2007. Imaging recollection and familiarity in the medial temporal lobe: a three-component model. Trends Cogn. Sci. 11 (9), 379–386. http://dx.doi.org/10.1016/j.tics.2007.08.001.
Fischl, B., 2012. FreeSurfer. NeuroImage 62 (2), 774–781. http://dx.doi.org/10.1016/j.neuroimage.2012.01.021.
Ghuman, A.S., Bar, M., Dobbins, I.G., Schnyer, D.M., 2008. The effects of priming on frontal-temporal communication. Proc. Natl. Acad. Sci. U. S. A. 105 (24), 8405–8409. http://dx.doi.org/10.1073/pnas.0710674105.

Ghuman, A.S., Brunet, N.M., Li, Y., Konecky, R.O., Pyles, J.A., Walls, S.A., ... Richardson, R.M., 2014. Dynamic encoding of face information in the human fusiform gyrus. Nat. Commun. 5, 5672. http://dx.doi.org/10.1038/ncomms6672.

Gillund, G., Shiffrin, R.M., 1984. A retrieval model for both recognition and recall. Psychol. Rev. 91 (1), 1–67.

Gonsalves, B.D., Kahn, I., Curran, T., Norman, K.A., Wagner, A.D., 2005. Memory strength and repetition suppression: multimodal imaging of medial temporal cortical contributions to recognition. Neuron 47 (5), 751–761. http://dx.doi.org/10.1016/j.neuron.2005.07.013.

Gramfort, A., Luessi, M., Larson, E., Engemann, D.A., Strohmeier, D., Brodbeck, C., ... Hämäläinen, M.S., 2014. MNE software for processing MEG and EEG data. NeuroImage 86, 446–460. http://dx.doi.org/10.1016/j.neuroimage.2013.10.027.

Hadoush, H., Sunagawa, T., Nakanishi, K., Endo, K., Ochi, M., 2011. Motor somatotopy of extensor indicis proprius and extensor pollicis longus. Neuroreport 22 (11), 559–564. http://dx.doi.org/10.1097/WNR.0b013e328348e750.

Hansen, P.C., Kringelbach, M.L., Salmelin, R., 2010. MEG. Oxford University Press, An introduction to methods.

Hastie, T., Tibshirani, R., Friedman, J., 2001. The Elements of Statistical Learning. Springer-Verlag, New York.

Hauk, O., Pulvermüller, F., 2004. Effects of word length and frequency on the human event-related potential. Clin. Neurophysiol. 115 (5), 1090–1103.

Hauk, O., Davis, M.H., Ford, M., Pulvermüller, F., Marslen-Wilson, W.D., 2006. The time course of visual word recognition as revealed by linear regression analysis of ERP data. NeuroImage 30 (4), 1383–1400. http://dx.doi.org/10.1016/j.neuroimage.2005.11.048.

Hauk, O., Pulvermüller, F., Ford, M., Marslen-Wilson, W.D., Davis, M.H., 2009. Can I have a quick word? Early electrophysiological manifestations of psycholinguistic processes revealed by event-related regression analysis of the EEG. Biol. Psychol. 80 (1), 64–74. http://dx.doi.org/10.1016/j.biopsycho.2008.04.015.

Haynes, J.-D., Rees, G., 2006. Decoding mental states from brain activity in humans. Nat. Rev. Neurosci. 7 (7), 523–534. http://dx.doi.org/10.1038/nrn1931.

Heil, M., Rösler, F., Hennighausen, E., 1997. Topography of brain electrical activity dissociates the retrieval of spatial versus verbal information from episodic long-term memory in humans. Neurosci. Lett. 222 (1), 45–48.

Henson, R.N., 2005. A mini-review of fMRI studies of human medial temporal lobe activity associated with recognition memory. Q. J. Exp. Psychol. B 58 (3–4), 340–360. http://dx.doi.org/10.1080/02724990444000113.

Hintzman, D.L., 1988. Judgments of frequency and recognition memory in a multiple-trace memory model. Psychol. Rev. 95 (4), 528–551. http://dx.doi.org/10.1037/0033-295X.95.4.528.

Hirshorn, E.A., Li, Y., Ward, M.J., Richardson, R.M., Fiez, J.A., Ghuman, A.S., 2016. Decoding and disrupting left midfusiform gyrus activity during word reading. Proc. Natl. Acad. Sci. U. S. A. 201604126. http://dx.doi.org/10.1073/pnas.1604126113.

Indefrey, P., Kleinschmidt, A., Merboldt, K.D., Krüger, G., Brown, C., Hagoort, P., Frahm, J., 1997. Equivalent responses to lexical and nonlexical visual stimuli in occipital cortex: a functional magnetic resonance imaging study. NeuroImage 5 (1), 78–81. http://dx.doi.org/10.1006/nimg.1996.0232.

Inoue, K., Nakanishi, K., Hadoush, H., Kurumadani, H., Hashizume, A., Sunagawa, T., Ochi, M., 2013. Somatosensory mechanical response and digit somatotopy within cortical areas of the postcentral gyrus in humans: an MEG study. Hum. Brain Mapp. 34 (7), 1559–1567. http://dx.doi.org/10.1002/hbm.22012.

Juhasz, B.J., Rayner, K., 2003. Investigating the effects of a set of intercorrelated variables on eye fixation durations in reading. J. Exp. Psychol. Learn. Mem. Cogn. 29 (6), 1312–1318. http://dx.doi.org/10.1037/0278-7393.29.6.1312.

Khader, P., Knoth, K., Burke, M., Ranganath, C., Bien, S., Rösler, F., 2007. Topography and dynamics of associative long-term memory retrieval in humans. J. Cogn. Neurosci. 19 (3), 493–512. http://dx.doi.org/10.1162/jocn.2007.19.3.493.

Lepage, M., Brodeur, M., Bourgouin, P., 2003. Prefrontal cortex contribution to associative recognition memory in humans: an event-related functional magnetic resonance imaging study. Neurosci. Lett. 346 (1–2), 73–76. http://dx.doi.org/10.1016/S0304-3940(03)00578-0.

Malmberg, K.J., 2008. Recognition memory: a review of the critical findings and an integrated theory for relating them. Cogn. Psychol. 57 (4), 335–384. http://dx.doi.org/10.1016/j.cogpsych.2008.02.004.

Maris, E., Oostenveld, R., 2007. Nonparametric statistical testing of EEG- and MEG-data. J. Neurosci. Methods 164 (1), 177–190. http://dx.doi.org/10.1016/j.jneumeth.2007.03.024.

Mitchell, K.J., Johnson, M., Raye, C.L., Greene, E.J., 2004. Prefrontal cortex activity associated with source monitoring in a working memory task. J. Cogn. Neurosci. 16 (6), 921–934. http://dx.doi.org/10.1162/0898929041502724.

Murdock, B.B., 1993. TODAM2: a model for the storage and retrieval of item, associative, and serial-order information. Psychol. Rev. 100 (2), 183–203. http://dx.doi.org/10.1037/0033-295X.100.2.183.

Nijboer, M., Borst, J.P., Van Rijn, H., Taatgen, N.A., 2016. Contrasting single and multi-component working-memory systems in dual tasking. Cogn. Psychol. 86, 1–26. http://dx.doi.org/10.1016/j.cogpsych.2016.01.003.

Norman, K.A., Polyn, S.M., Detre, G.J., Haxby, J.V., 2006. Beyond mind-reading: multi-voxel pattern analysis of fMRI data. Trends Cogn. Sci. 10 (9), 424–430. http://dx.doi.org/10.1016/j.tics.2006.07.005.

Nyhus, E., Curran, T., 2009. Semantic and perceptual effects on recognition memory: evidence from ERP. Brain Res. 1283, 102–114. http://dx.doi.org/10.1016/j.brainres.2009.05.091.

Oostenveld, R., Fries, P., Maris, E., Schoffelen, J.-M., 2011. FieldTrip: open source software for advanced analysis of MEG, EEG, and invasive electrophysiological data. Comput. Intell. Neurosci. 2011 (1), 1–9. http://dx.doi.org/10.1016/j.neuroimage.2009.02.041.

Pereira, F., Mitchell, T., Botvinick, M., 2009. Machine learning classifiers and fMRI: a tutorial overview. NeuroImage 45 (1), S199–S209. http://dx.doi.org/10.1016/j.neuroimage.2008.11.007.

Pisoni, A., Turi, Z., Raithel, A., Ambrus, G.G., Alekseichuk, I., Schacht, A., ... Antal, A., 2015. Separating recognition processes of declarative memory via anodal tDCS: boosting old item recognition by temporal and new item detection by parietal stimulation. PLoS One 10 (3), e0123085. http://dx.doi.org/10.1371/journal.pone.0123085.

Rotello, C.M., Heit, E., 2000. Associative recognition: a case of recall-to-reject processing. Mem. Cogn. 28 (6), 907–922. http://dx.doi.org/10.3758/BF03209339.

Rotello, C.M., Macmillan, N.A., Van Tassel, G., 2000. Recall-to-reject in recognition: evidence from ROC curves. J. Mem. Lang. 43 (1), 67–88. http://dx.doi.org/10.1006/jmla.1999.2701.

Rugg, M.D., Curran, T., 2007. Event-related potentials and recognition memory. Trends Cogn. Sci. 11 (6), 251–257. http://dx.doi.org/10.1016/j.tics.2007.04.004.

Rugg, M.D., Yonelinas, A.P., 2003. Human recognition memory: a cognitive neuroscience perspective. Trends Cogn. Sci. 7 (7), 313–319.

Rugg, M.D., Henson, R.N.A., Robb, W.G.K., 2003. Neural correlates of retrieval processing in the prefrontal cortex during recognition and exclusion tasks. Neuropsychologia 41 (1), 40–52. http://dx.doi.org/10.1016/S0028-3932(02)00129-X.

Schneider, D.W., Anderson, J.R., 2012. Modeling fan effects on the time course of associative recognition. Cogn. Psychol. 64 (3), 127–160. http://dx.doi.org/10.1016/j.cogpsych.2011.11.001.

Sohn, M.H., Goode, A., Stenger, V.A., Carter, C.S., Anderson, J.R., 2003. Competition and representation during memory retrieval: roles of the prefrontal cortex and the posterior parietal cortex. Proc. Natl. Acad. Sci. U. S. A. 100 (12), 7412–7417. http://dx.doi.org/10.1073/pnas.0832374100.

Sohn, M.H., Goode, A., Stenger, V.A., Jung, K.J., Carter, C.S., Anderson, J.R., 2005. An information-processing model of three cortical regions: evidence in episodic memory retrieval. NeuroImage 25 (1), 21–33. http://dx.doi.org/10.1016/j.neuroimage.2004.11.001.

Speer, N.K., Curran, T., 2007. ERP correlates of familiarity and recollection processes in visual associative recognition. Brain Res. 1174, 97–109. http://dx.doi.org/10.1016/j.brainres.2007.08.024.

Spinelli, D., De Luca, M., Di Filippo, G., Mancini, M., Martelli, M., Zoccolotti, P., 2005. Length effect in word naming in reading: role of reading experience and reading deficit in Italian readers. Dev. Neuropsychol. 27 (2), 217–235. http://dx.doi.org/10.1207/s15326942dn2702_2.

Stark, C.E., Squire, L.R., 2001. Simple and associative recognition memory in the hippocampal region. Learn. Mem. 8 (4), 190–197. http://dx.doi.org/10.1101/lm.40701.

Sudre, G., Pomerleau, D., Palatucci, M., Wehbe, L., Fyshe, A., Salmelin, R., Mitchell, T., 2012. Tracking neural coding of perceptual and semantic features of concrete nouns. NeuroImage 62 (1), 451–463. http://dx.doi.org/10.1016/j.neuroimage.2012.04.048.

Van Petten, C., Kutas, M., 1990. Interactions between sentence context and word frequency in event-related brain potentials. Mem. Cogn. 18 (4), 380–393.

Wixted, J.T., 2007. Dual-process theory and signal-detection theory of recognition memory. Psychol. Rev. 114 (1), 152.

Wixted, J.T., Stretch, V., 2004. In defense of the signal detection interpretation of remember/know judgments. Psychon. Bull. Rev. 11 (4), 616–641. http://dx.doi.org/10.3758/BF03196616.

Yonelinas, A.P., 2002. The nature of recollection and familiarity: a review of 30 years of research. J. Mem. Lang. 46 (3), 441–517. http://dx.doi.org/10.1006/jmla.2002.2864.